DETRENDED TOPOGRAPHIC DATA OF THE SOUTH-POLE AITKEN BASIN (SPA): COMPARISONS WITH APOLLO 16 AND SCHILLER-SCHICKARD AS INDICATIONS OF THE FORMATION AND EVOLUTION OF THE SPA INTERIOR. N. E. Petro[1], D. Hollibaugh-Baker[1], and B. L. Jolliff[2], [1]NASA Goddard Space Flight Center, Planetary Geology, Geophysics, and Geochemistry Lab, Code 698, Greenbelt, MD 20771, [2]Department of Earth and Planetary Sciences, Washington University, St. Louis, MO 63130 (Noah.E.Petro@nasa.gov).

Introduction: Data from recent lunar orbital missions have provided critical insight into the surface composition, morphology, and geologic history of the Moon. A key region that has benefited from this new data is the South Pole-Aitken Basin (SPA), a key area for future sample return [1, 2]. A key area of investigation of SPA has been the characterization of its surface, detailing the interior composition [3, 4], geologic evolution [5, 6], and possible exposure of deep-seated materials [7, 8]. Recently we have applied a number of datasets to ascertain the origin of surfaces in central SPA and identify units that represent the ancient SPA-derived impact melt and those that represent volcanic activity [9, 10]. Here we apply a technique that utilizes high-resolution topographic data to remove local slopes to highlight subtle topographic variations [11]. Such detrended data allows us to characterize units that are either ancient (SPA impact melt) or that represent subsequent volcanic activity.

Detrended Topography: Recent work by Kreslavsky *et al*. [11] has shown that very subtle (*i.e*., features with low topographic amplitude) volcanic and structural features become readily apparent in detrended data. The approach calculates the median elevation of neighboring pixels and subtracts that median elevation from a central pixel. The major difference between the approach used by Kreslavsky *et al*. and what we use here is that we calculate the median neighboring topography in a 10x10 box, instead of a circle. This difference does not cause any significant difference in the interpretation of the detrended data. Using the detrended data (at 64 pixels per degree, ~474 mpp) from LOLA results maps that aid in the delineation of surface units. We will also explore other higher-resolution topographic datasets, specifically the joint Selene-LOLA product [12] and from LROC NAC DTM's [13, 14].

Case Studies: To illustrate what the detrended data show, we explore two "type-localities" of impact and volcanic modified surfaces, the Apollo 16 landing site and the Schiller-Schickard region.

Apollo 16. The Apollo 16 landing site is in an area dominated by impact debris from nearby impact basins and large craters [15]. The detrended topography (Fig. 1) illustrates the change in local slopes that occurs between the Cayley Formation (west of the landing site) and the Descartes Mountain Formation [16] (east of the landing site). What this illustrates, unsurprisingly, is that the filled craters (*e.g.*, Dolland B, Fig. 1) are smoother than the surrounding ancient highlands at the 100's of meters scale. This delineation of units is useful for characterizing basin and crater-related deposits within central SPA [17].

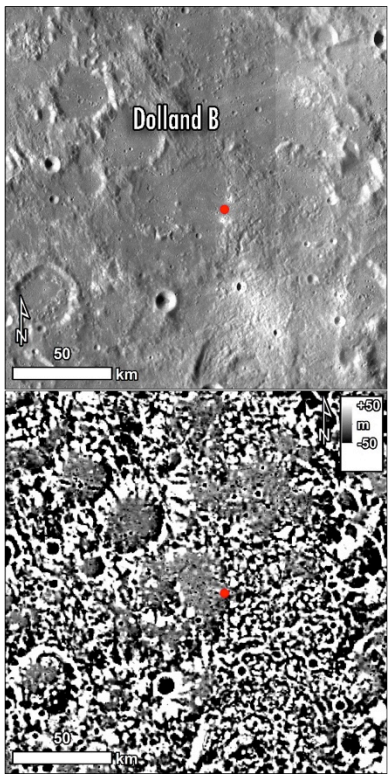

Figure 1. LROC WAC mosaic (top) and LOLA detrended topography (bottom) of the Apollo 16 landing site region (landing site marked by red dot). Detrended topography illustrates elevation change relative to the local median topography [11].

Schiller-Schickard. The Schiller-Schickard region is characterized by the presence of ancient basalts that are coated in a thin veneer of crater ejecta [18]. The increased albedo and dark-haloed craters, coupled with enhancements in iron within the deposits, are hallmarks of these ejecta-volcanic units [e.g., 19]. Similar regions are observed across the Moon, and have been mapped as occurring within central SPA [6, 20]. The detrended topography of Schiller-Schickard clearly shows that the area of cryptomare within Schickard is similar to the volcanic surfaces, suggesting that the emplacement of

ejecta did not alter the topography of the surface over the 100s of meters of horizontal scale. Additionally, nearby crater interiors are also relatively smooth, but contain morphologic indications of volcanic activity (*e.g.,* lava flows and wrinkle ridges).

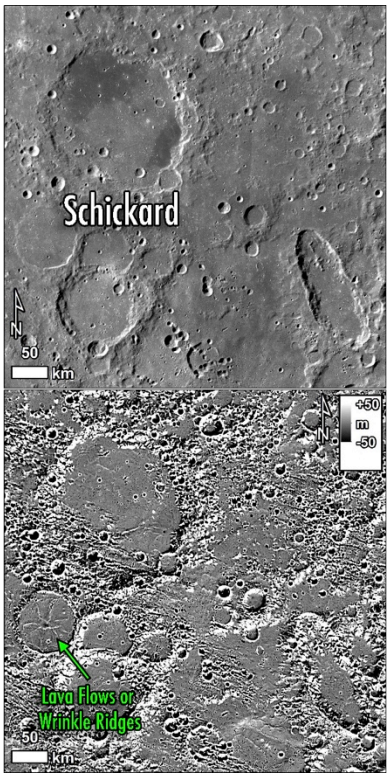

Figure 2. LROC WAC mosaic (top) and LOLA detrended topography (bottom) of the Schiller-Schickard region. Subtle lava flows or wrinkle ridges that are apparent in the detrended topography (bottom) that are not clear in images alone.

Topography of the Interior of SPA: The interior of SPA contains a variety of geologic units [21-23], and disentangling the volcanic, impact ejecta-related, and ancient impact-melt surfaces is key to interpreting the geologic evolution of the basin [4]. The detrended topography of the region surrounding Bhabha crater (Fig. 3) clearly shows the signature of smooth volcanic fill and the rugged morphology associated with ancient surfaces (some of which may be volcanic [4]). The boundary between these two units is typically sharp, but in places grade gradually over 10s of km (Fig. 3). While these differences are apparent in images (Fig. 3 top) and in other remote sensing datasets [3, 21], what is apparent are the boundaries of these units, which are difficult to discern in other data. However, if there are extensive cryptomare deposits in this region, particularly to the east of Bhabha [6], they are manifested distinctly from what is observed at Schiller-Schickard (Fig. 2).

Conclusions: Detrended topographic data provide a quantifiable method for enhancing and highlighting subtle morphologic changes over various baselines. The surface expression of volcanism, crater and basin ejecta deposits, and structural features are enhanced in the detrended data [11]. This analysis is useful for guiding further investigations into the origin and age of surface units, integration with other complementary data [14], as part of ongoing efforts to unravel the geologic history of the interior of SPA basin.

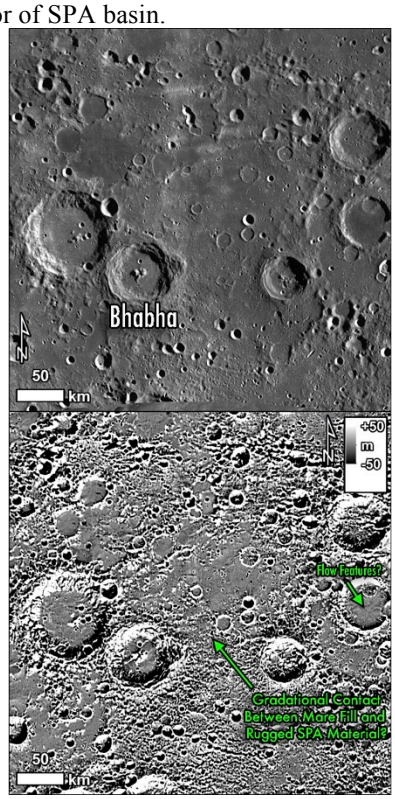

Figure 3. LROC WAC mosaic (top) and LOLA detrended topography of central SPA, near Bhabha crater.

References: [1] Planetary Science Decadal Survey, (2011). [2] Jolliff, B., et al., (2017), *LPSC 48*, Abst. #1300. [3] Borst, A. M., et al., (2012) *Planetary and Space Science*, 68, 76-85. [4] Moriarty, D. P. and C. M. Pieters, (2016) LPSC 47, 1735. [5] Hurwitz, D. M. and D. A. Kring, (2014) *Journal of Geophysical Research: Planets*, 119, 2013JE004530. [6] Whitten, J. L. and J. W. Head, (2015) *Icarus*, 247, 150-171. [7] Klima, R. L., et al., (2011) *Journal of Geophysical Research*, 116, [8] Yamamoto, S., et al., (2012) *Icarus*, 218, 331-344. [9] Petro, N., (2015), *NASA ESF*. [10] Petro, N. E., et al., (2016), LPSC 47, 2669. [11] Kreslavsky, M. A., et al., (2017) *Icarus*, 283, 138-145. [12] Barker, M. K., et al., (2016) *Icarus*, 273, 346-355. [13] Henriksen, M. R., et al., (2017) *Icarus*, 283, 122-137. [14] Lawrence, S. J., et al., (2016) LPSC 47, 2755. [15] Hodges, C. A., et al., (1973) *Proc. Lunar Sci. Conf.*, 4th, 1-25. [16] Milton, D., (1972) 1:250,000 Geologic Map of the Descartes Region of the Moon: Apollo 16 Pre-Mission Map (1-748A), [17] Petro, N. E. and C. M. Pieters, (2004) *Journal of Geophysical Research*, 109(E6), E06004, doi:06010.01029/02003JE002182. [18] Blewett, D. T., et al., (1995) *JGR*, 100, 16959-16978. [19] Hawke, B. R. and J. F. Bell, (1982), *Proc. Lunar Sci. Conf.*,Abst. #665-678. [20] Schultz, P. H. and P. D. Spudis, (1979) *Proc. Lunar Sci. Conf.*, 10, 2899-2918. [21] Petro, N. E., et al., (2011), doi:10.1130/2011.2477(1106). [22] Stuart-Alexander, D. E., (1978) Geologic map of the central far side of the Moon, I-1047. [23] Pieters, C. M., et al., (2001) *JGR*, 106, 28001-28022.